47th AIAA Aerospace Sciences Meeting Including The New Horizons Forum and Aerospace Exposition
5 - 8 January 2009, Orlando, Florida

AIAA 2009-476

Falkner-Skan flow over a wedge with slip boundary conditions

Michael J. Martin[1] and Iain D. Boyd[2]
University of Michigan, Ann Arbor, MI 48109-2140

     The Falkner-Skan solution for laminar boundary layer flow over a wedge is modified to allow for a slip boundary condition. A modified boundary layer Knudsen number K is introduced, and the coordinate system is transformed from one-dimensional to two-dimensional to allow for the loss of self-similarity in the flow. A marching scheme is used to solve the boundary layer equations in the rarefied flow regime. The results of this solution show decreased skin friction, boundary layer thickness, velocity thickness, and momentum thickness due to the presence of the slip boundary condition. When the energy equation is solved using a temperature jump boundary condition, the heat transfer increases for slightly rarefied flows, and then decreases as the Knudsen number increases.

Nomenclature

b	=	velocity coefficient
c_p	=	specific heat
f	=	non-dimensional stream function
m	=	flow exponent
n	=	distance in the normal direction
K	=	non-equilibrium parameter
Kn	=	Knudsen number
P	=	pressure
Pr	=	Prandtl number
Re	=	Reynolds number
T	=	temperature
U	=	external x-velocity
u	=	x-velocity
v	=	y-velocity
x	=	position in the flow direction
y	=	position in the flow normal direction
α	=	thermal diffusivity
β	=	included angle
γ	=	specific heat ratio
δ	=	boundary layer thickness
δ^*	=	displacement thickness
η	=	non-dimensional position
θ	=	momentum thickness
λ	=	mean-free path
μ	=	viscosity
ρ	=	density
σ	=	accommodation coefficient
τ	=	shear stress
υ	=	kinematic viscosity

---

[1] Graduate Student Research Assistant, Department of Aerospace Engineering, AIAA member. Current address: Department of Mechanical Engineering, Louisiana State University, Baton Rouge, LA 70703.
[2] Professor, Department of Aerospace Engineering, AIAA Associate Fellow.

Subscripts

g   =   gas
M   =   momentum
o   =   free-stream
slip   =   slip
T   =   thermal
w   =   wall

Superscripts

*   =   non-dimensional

I.   Introduction

THE solution of the laminar boundary layer equations under rarefied flow conditions at low Mach numbers has applications to several areas of engineering interest, including aerosol science,[1] subsonic flight in extraterrestrial atmospheres,[2] and micro- and nano- air vehicles.[3-4] Initial attempts to solve the boundary layer equations with a slip boundary condition using perturbation methods[5-6] suggested that the slip condition would not affect shear stress, boundary layer thickness, or heat transfer. A later, more complete, thermal analysis using similar methods[7] partially contradicted this result, suggesting that heat transfer was changed by the presence of a slip boundary condition. The apparent lack of a change in shear stress due to the slip condition led to the conclusion that the terms added by the slip boundary condition were smaller than the discarded second order terms in the boundary layer equations.[8-9] This, in turn, led to the conclusion that slip could be ignored in a laminar boundary layer.

Complete numerical solutions of the Blasius boundary layer equations with slip flow over a flat plate[10] and stagnation point flow[11] contradicted the conclusion that slip did not change shear stress within a laminar boundary layer. This analysis showed that the slip condition changes the boundary layer structure from a self-similar profile to a two-dimensional structure, which can be non-dimensionalized using a boundary layer Knudsen number. This solution showed decreased shear stress, boundary layer thickness, and heat transfer. The loss of self-similarity was consistent with trends observed in other rarefied flows, such as slip flow in micro-channels.[12-13]

The Blasius boundary layer solution[14] is only one member of a larger family of boundary layer solutions known as Falkner-Skan flow.[15-16] The boundary layer equations for Falkner-Skan flow apply to two-dimensional flow over a wedge with an included angle of $\beta\pi$, and an external pressure gradient based on the inviscid flow solution. A value of β of zero corresponds to the flat-plate Blasius solution, and a value of 1 corresponds to a stagnation region.

The present work adds a slip-flow boundary condition to the Falkner-Skan equations, allowing the fluid flow and heat transfer to be determined for a wedge in moderately rarefied flow. The boundary layer momentum and energy equations for slip flow over a wedge are derived. A marching scheme to solve these equations is outlined. Numeric solutions are provided for flow and heat transfer over several wedge half-angles, with discussion of these results.

II.   Formulation of the Governing Equations

Because of the loss of self-similarity, the non-dimensional x-momentum and thermal transport equations must be re-formulated to incorporate variation in the x-direction. This requires extending non-dimensionalizations previously used for the flat plate in slip flow[10] to incorporate wedge flow.

A. The Momentum Equation

As shown in Figure 1, flow over the top of a wedge can be modeled as an external flow U(x) with a pressure gradient given by the inviscid flow solution. The angle of the wedge is given as $\beta\pi$.
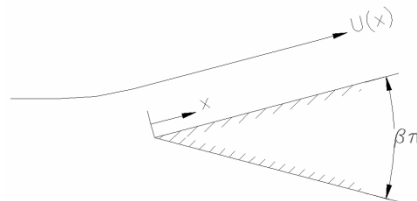

Figure 1. Boundary Layer Flow Over a Wedge

The external flow velocity and pressure gradients are given by:

$$U(x) = bx^m \tag{1}$$

$$\frac{\partial P}{\partial x} = -\rho U(x)\frac{dU(x)}{dx} = -m\rho b^2 x^{2m-1} \tag{2}$$

where U is the external velocity, P is the pressure, ρ is the density, and x is the position along the wedge. The coefficient b is a function of the flow geometry. As long as the boundary layer is relatively thin, the external flow, and the pressure gradient will be independent of the thickness of the boundary layer.

The exponent m is a function of the angle β:

$$m = \frac{\beta}{2-\beta}. \tag{3}$$

The flow near the wedge will be governed by the boundary layer equations. The equation for continuity is identical to the flat-plate case:

$$\frac{\partial u}{\partial x} + \frac{\partial v}{\partial y} = 0 \tag{4}$$

For steady flow in a boundary layer, the x-momentum equation is given by:

$$u\frac{\partial u}{\partial x} + v\frac{\partial u}{\partial y} = -\frac{1}{\rho}\frac{dP(x)}{dx} + \upsilon\frac{\partial^2 u}{\partial y^2} \tag{5}$$

where u is the x-velocity, v is the y velocity, and υ is the kinematic viscosity.

These equations can then be transformed, using the non-dimensionalizations and non-dimensional stream functions developed by Falkner and Skan. These non-dimensionalizations are similar to, but not identical to, those used by Blasius. A non-dimensional flow coordinate η is formed by combining x and y with the other flow variables:

$$\eta = y\sqrt{\frac{m+1}{2}\frac{b}{\upsilon}}x^{\frac{m-1}{2}}. \tag{6}$$

A non-dimensional stream function f(η) is found from the dimensional stream function ψ:

$$\psi(x,y) = \sqrt{\frac{2b\upsilon}{m+1}}x^{\frac{m+1}{2}}f(\eta). \tag{7}$$

The non-dimensional velocities are given as:

$$u^* = \frac{u}{U(x)} = f'(\eta) \tag{8}$$

$$v^* = \frac{v}{\sqrt{\frac{2}{m+1}\upsilon bx^{m-1}}} = \left[f(\eta) - \frac{m-1}{m+1}\eta f'(\eta) \right]. \tag{9}$$

A governing equation for f can be found by substituting these non-dimensional terms into the x-momentum equation (5):

$$f'''(\eta) + f(\eta)f'(\eta) + \beta(1-(f'(\eta))^2) = 0. \tag{10}$$

For the no-slip case, the boundary conditions are:

$$u^*(y=0) = 0 \Rightarrow f'(\eta = 0) = 0 \tag{11}$$

$$v*(y=0)=0 \Rightarrow f(\eta=0)=0 \tag{12}$$

$$u*(y \to \infty)=1 \Rightarrow f'(\eta \to \infty)=1. \tag{13}$$

For slightly rarefied flows, the no-slip boundary condition (11) is replaced by a slip condition.[17]

$$u_{slip} = u_g - u_w = \lambda \frac{2-\sigma_M}{\sigma_M} \left.\frac{\partial u}{\partial n}\right|_{wall} + \frac{3}{4}\frac{\upsilon}{T_g}\left.\frac{\partial T}{\partial s}\right|_{wall} \tag{14}$$

where u_{slip} is the wall slip velocity, u_g is the gas velocity at the wall, u_w is the wall velocity, $\partial u/\partial n$ is the velocity gradient normal to the wall, λ is the mean free path of the gas, σ_M is the tangential momentum accommodation coefficient, ρ is the density of the gas, T_g is the temperature of the gas, and $\partial T/\partial s$ is the temperature gradient along the wall.

For an isothermal wall, equation (14) can be non-dimensionalized to obtain:

$$\left.\frac{\partial f}{\partial \eta}\right|_{\eta=0} = \frac{(2-\sigma_M)}{\sigma_M}\sqrt{\frac{m+1}{2}}\frac{\lambda}{x}\sqrt{\frac{xU(x)}{\upsilon}}\left.\frac{\partial^2 f}{\partial \eta^2}\right|_{\eta=0} = K\left.\frac{\partial^2 f}{\partial \eta^2}\right|_{\eta=0}. \tag{15}$$

The non-equilibrium parameter K, which is proportional to the boundary layer Knudsen number, is defined as:

$$K = \frac{(2-\sigma_M)}{\sigma_M}\sqrt{\frac{m+1}{2}}\frac{\lambda}{x}\sqrt{\frac{xU(x)}{\upsilon}} = \frac{(2-\sigma_M)}{\sigma_M}\sqrt{\frac{m+1}{2}}\lambda\sqrt{\frac{b}{\upsilon}}x^{\frac{m-1}{2}}$$

$$= \frac{(2-\sigma_M)}{\sigma_M}\sqrt{\frac{m+1}{2}}Kn_x \, Re_x^{1/2} \tag{16}$$

where Kn_x and Re_x are the Knudsen and Reynolds numbers based on x.

Just as in the flat plate case, the revised boundary condition leads to a loss of self-similarity, and the velocity will be a function of both η and K. While the definition of $u*$ is unchanged, the definition of $v*$ must be modified to incorporate the derivative of the stream function with respect to K. The revised definition of $v*$ is

$$v* = \frac{v}{(\upsilon U(x)/x)^{1/2}} = -\left[\frac{m-1}{m+1}\left(\eta\frac{\partial f(\eta,K)}{\partial \eta}+K\frac{\partial f(\eta,K)}{\partial K}\right)+f(\eta,K)\right]. \tag{17}$$

When all other derivatives in x are re-written to include a K term, the ordinary differential equation given in (10) is replaced by a partial differential equation:

$$\frac{\partial^3 f}{\partial \eta^3}+f\frac{\partial^2 f}{\partial \eta^2}+\beta\left(1-\left(\frac{\partial f}{\partial \eta}\right)^2\right)+K(1-\beta)\frac{\partial}{\partial \eta}\left[\frac{\partial f}{\partial \eta}\frac{\partial f}{\partial K}\right]=0. \tag{18}$$

Equation (18) requires boundary conditions in K. As K approaches zero, the no-slip result will be recovered. At large values of K, the Navier-Stokes equations, and the continuum hypothesis, will have broken down, and free-molecular flow will result. This will result in a uniform velocity u, and full slip at the wall. The boundary conditions then become

$$\left.\frac{\partial f}{\partial \eta}\right|_{K \to \infty} = 1 \tag{19}$$

$$f(K \to \infty)=\eta. \tag{20}$$

B. The Energy Equation

The equation for conservation of energy in a boundary layer with steady flow is given as:

$$u \frac{\partial T}{\partial x} + v \frac{\partial T}{\partial y} = \frac{\alpha}{\rho c_p} \frac{\partial^2 T}{\partial y^2} . \tag{21}$$

where T is the local temperature, α is the thermal diffusivity of the gas, and c_p is the specific heat of the fluid.[18]
The temperature can be non-dimensionalized as

$$T^* = \frac{T - T_w}{T_o - T_w} . \tag{22}$$

where T_o is the free-stream temperature and T_w is the surface temperature.
Using the non-dimensionalizations used for the fluid flow equations, and the non-dimensional temperature, the heat equation becomes:

$$\frac{\partial^2 T^*}{\partial \eta^2} + \Pr f \frac{\partial T^*}{\partial \eta} + K \Pr (1 - \beta) \left[\frac{\partial f}{\partial \eta} \frac{\partial T^*}{\partial K} + \frac{\partial f}{\partial K} \frac{\partial T^*}{\partial \eta} \right] = 0 . \tag{23}$$

where Pr is the Prandtl number of the fluid.
For rarefied flows, a thermal jump condition will occur at the wall:

$$T_{gas} - T_w = \frac{\lambda}{\Pr} \frac{2 - \sigma_T}{\sigma_T} \frac{2\gamma}{\gamma + 1} \frac{\partial T}{\partial n} \bigg|_{wall} . \tag{24}$$

where T_{gas} is the temperature of the gas at the wall, σ_T is the thermal accommodation coefficient, and γ is the specific heat ratio.[19]   This expression can be non-dimensionalized to obtain

$$T^*(\eta = 0) = \frac{1}{\Pr} \frac{2 - \sigma_T}{\sigma_T} \frac{2\gamma}{\gamma + 1} \sqrt{\frac{m+1}{2}} \; \lambda \sqrt{\frac{b}{\upsilon}} x^{\frac{m-1}{2}} \frac{\partial T^*}{\partial \eta} \bigg|_{wall} . \tag{25}$$

If the thermal and momentum accommodation coefficients are assumed to be approximately equal, this expression simplifies to:

$$T^*(\eta = 0) = \frac{1}{\Pr} \frac{2\gamma}{\gamma + 1} K \frac{\partial T^*}{\partial \eta} \bigg|_{wall} . \tag{26}$$

At large values of y, the temperature will approach the free-stream value, giving the boundary condition:

$$T^*(\eta = \infty) = 1 . \tag{27}$$

At large values of K, the temperature jump will become large, and a uniform temperature profile will result, giving the boundary condition:

$$T^*(K \to \infty) = 1 . \tag{28}$$

As K approaches 0, the no-slip solution should be recovered.

III.   Numeric Formulation

The loss of self-similarity means that the boundary layer must be solved as a partial differential equation instead of an ordinary differential equation. Equations (18) and (23) can be solved using a modified boundary-layer solver. Because large values of K correspond to small values of x, the solver begins from large values of K, and marches towards a K of zero, going from non-equilibrium flows to equilibrium conditions in the process. This corresponds to the process used in standard boundary layer codes, only in non-dimensional coordinates.[20]
Equation (18) can be simplified by replacing $\partial f / \partial \eta$ with f':

$$\frac{\partial^2 f'}{\partial \eta^2} + f \frac{\partial f'}{\partial \eta} + \beta \left(1 - (f')^2 \right) + K(1 - \beta) \frac{\partial}{\partial \eta} \left[f' \frac{\partial f}{\partial K} \right] = 0 . \tag{29}$$

f', and all its derivatives, are found using center-difference schemes:

$$f'_{i,j} = \frac{f_{i,j+1} - f_{i,j-1}}{2\Delta\eta} + O\left((\Delta\eta)^2\right). \tag{30}$$

$$\left.\frac{\partial f'}{\partial \eta}\right|_{i,j} = \frac{f'_{i,j+1} - f'_{i,j-1}}{2\Delta\eta} + O\left((\Delta\eta)^2\right). \tag{31}$$

$$\left.\frac{\partial^2 f'}{\partial \eta^2}\right|_{i,j} = \frac{f'_{i,j+1} - 2.0 f'_{i,j} + f'_{i,j-1}}{(\Delta\eta)^2} + O\left((\Delta\eta)^2\right). \tag{32}$$

The mixed derivative term is found using an upwind scheme:

$$\frac{\partial}{\partial\eta}\left[f'\frac{\partial f}{\partial K}\right]_{i,j} = \frac{1}{\Delta\eta}\frac{1}{\Delta K}\left[f'_{i,j}\left(f_{i,j} - f_{i-1,j}\right) - f'_{i,j-1}\left(f_{i,j-1} - f_{i-1,j-1}\right)\right]. \tag{33}$$

Combining (30) through (32) into (29) gives the following expression for f:

$$
\begin{aligned}
f_{i-1,j} = f_{i,j} &+ \frac{f'_{i,j-1}}{f'_{i,j}}\left(f_{i-1,j-1} - f_{i,j-1}\right) \\
&+ \frac{2\Delta K}{(1-\beta)K f'_{i,j}}\left(\frac{f'_{i,j+1} - 2.0 f'_{i,j} + f'_{i,j-1}}{\Delta\eta} + \frac{f_{i,j}}{4.0}\left(f'_{i,j+1} - f'_{i,j-1}\right) + \frac{\beta\Delta\eta}{2}\left(1 - (f'_{i,j})^2\right)\right)
\end{aligned}
\tag{34}
$$

The slip condition is implemented using the following:

$$f'_{i,1} = \frac{K_i f'_{i,2}}{\left(K_i + \Delta\eta_{wall}\right)} + O\left(\frac{(\Delta\eta)^2}{(\Delta\eta + K_i)}\right)\frac{\partial^2 f'}{\partial\eta^2}. \tag{35}$$

Equations (12) and (13) provide the other required boundary conditions:

$$f_{i,1} = 0 \tag{36}$$

$$f_{i,m} = f_{i,m-1} + \Delta\eta. \tag{37}$$

Discretizing the energy equation is simpler. Using center-difference approximations in η, and an upwind scheme in K, the energy equation becomes:

$$
\begin{aligned}
T^*_{i-1,j} = T^*_{i,j} &+ \frac{(T^*_{i,j+1} - T^*_{i,j-1})(f_{i,j} - f_{i-1,j})}{2 f'_{i,j}\Delta\eta} \\
&+ \frac{\Delta K}{f'_{i,j} K \Pr(1-\beta)}\left[\frac{(T^*_{i,j+1} - 2.0 T^*_{i,j-1} + T^*_{i,j-1})}{(\Delta\eta)^2} + \Pr f_{i,j}\frac{(T^*_{i,j+1} - T^*_{i,j-1})}{2\Delta\eta}\right].
\end{aligned}
\tag{38}
$$

The wall temperature-jump boundary condition becomes:

$$T^*_{i,1} = \frac{\left(\dfrac{1}{\Pr}\dfrac{2\gamma}{\gamma+1}\right)}{\left(\dfrac{1}{\Pr}\dfrac{2\gamma}{\gamma+1}\right) + \Delta\eta} T^*_{i,2}. \tag{39}$$

The far-field boundary condition is given as

$$T^*_{i,m} = 1. \tag{40}$$

For the stagnation flow case, the momentum and energy equations are solved using a shooting method, just as is done for the no-slip formulation of Falkner-Skan flow.

IV.   Fluid Flow Results

Figures 2 and 3 show the non-dimensional wall slip velocity and wall shear stress as functions of K for half-angles of 15, 30, 45, 60, and 75 degrees. Previously reported values for a flat plate (0 degrees)[10] and a stagnation point (90 degrees)[11] are included for reference. These results suggest that slip effects are detectable at values of K below 1.0. They also suggest that the relative importance of slip effects increases with increasing wedge angle.
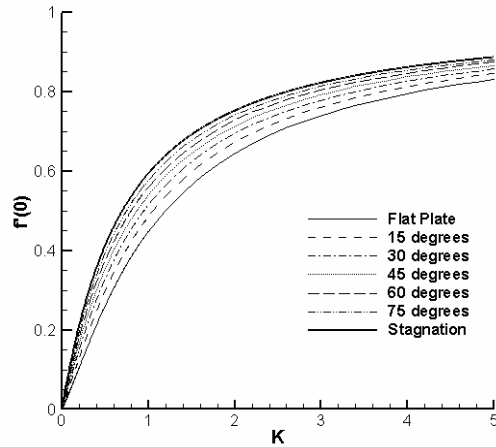
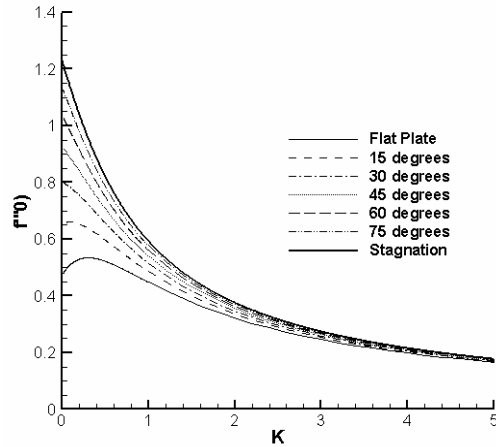Figure 2. Non-Dimensional Wall Velocity as a Function of K

Figure 3. Non-Dimensional Wall Friction as a Function of K

Figure 3 shows that for the flat plate, and 15-degree wedge, the maximum shear stress is encountered not at the equilibrium condition, but in slightly rarefied flow. This local minimum disappears as the wedge half-angle increases. This surprising result agrees with earlier analysis[10] of a flat-plate slip flow.

In addition to the shear stress, the boundary layer thickness, velocity thickness, and momentum thickness are quantities of interest in boundary layer flows.[16]   Figures 4, 5, and 6 show the boundary layer thickness, velocity thickness, and momentum thickness as functions of K for half-angles of 0, 15, 30, 45, 60, 75, and 90 degrees. These results show that the boundary layer thickness may decrease by 50 percent or more. The velocity thickness and momentum thickness may decrease by even larger amounts at high values of K. These results appear to be relatively independent of wedge half-angle.
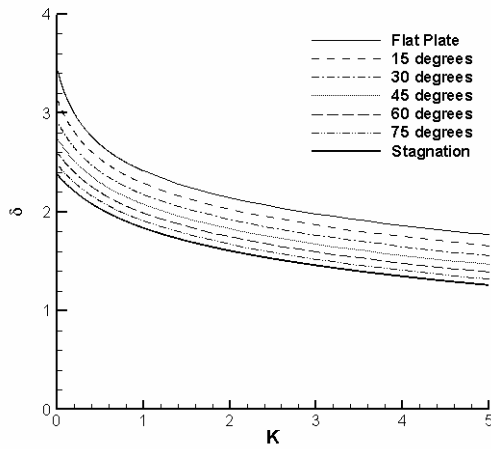
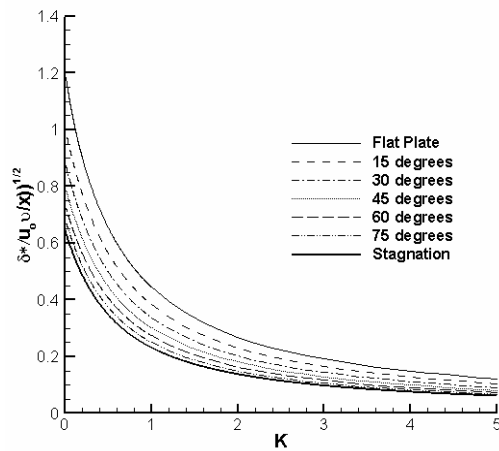Figure 4. Boundary Layer Thickness as a Function of K

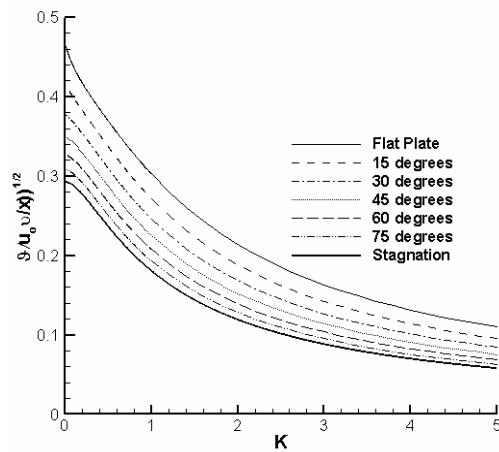Figure 5. Velocity Thickness as a Function of K

Figure 6. Momentum Thickness as a Function of K

V.   Heat Transfer Results

The heat-transfer is computed for a specific heat ratio of 1.4, representing a diatomic gas. Three representative Prandtl numbers are used: 0.7, 1.0, and 1.4, to determine the effect of changing the Prandtl number of the gas. Figure 7 shows the gas temperature at the wall as a function of K for wedge half-angles of 0, 30, and 60 degrees for a diatomic gas.   The increase in gas temperature at the wall due to rarefaction effects is largest for the flat plate

case, and decreases with increasing wedge half-angle. As expected from equation (26), the temperature jump decreases with increasing Prandtl number.
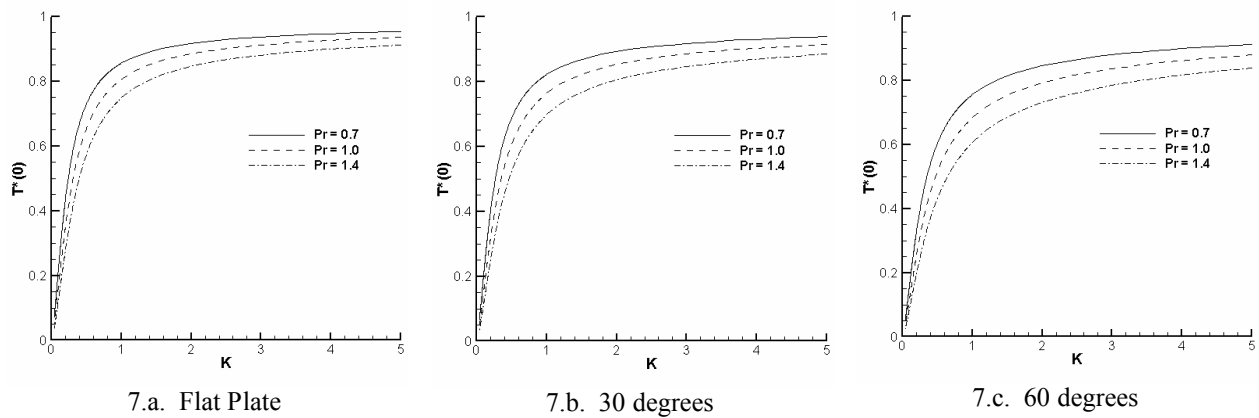

7.a. Flat Plate   7.b. 30 degrees   7.c. 60 degrees

Figure 7. Non-Dimensional Wall Temperature as a Function of K, γ=1.4 for Flat Plate, 30 degrees, and 60 degrees

Figure 8 shows the non-dimensionalized wall heat transfer as a function of K for wedge half-angles of 0, 30, and 60 degrees for diatomic gases. These results show a local maximum in the heat transfer at values of K of less than one for 0, 30, and 60 degrees. This result may be considered to be analogous to the local maximum in shear stress encountered earlier. The maximum moves to lower values of K with decreasing Prandtl numbers, and with increasing wedge half-angles. The local maximum disappears entirely in the stagnation flow condition.
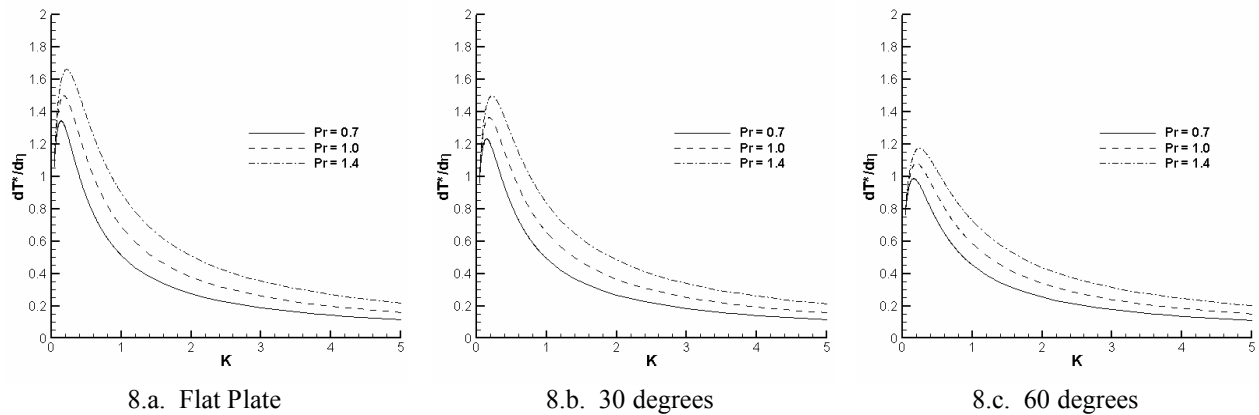

8.a. Flat Plate   8.b. 30 degrees   8.c. 60 degrees

Figure 8. Non-Dimensional Heat Transfer as a Function of K, γ=1.4 for Flat Plate, 30 degrees, and 60 degrees

The difference in heat transfer rates between slip-flow and non-slip flow cases increases with increasing Prandtl number. The increase in heat transfer appears to be slightly higher for the diatomic cases. Overall, the heat transfer increases by as much as 50 percent, or decreases by as much as 80 percent, from non-equilibrium values, depending on the flow conditions.

VI.   Conclusion

Slip flow over a wedge was analyzed incorporating a slip boundary condition. The non-dimensional governing equations used to compute the flow in the no-slip condition were modified to allow for the loss of self-similarity that accompanies the slip boundary condition.

Numeric solution of the modified boundary layer equations showed a local increase in skin friction under slightly rarefied conditions, and then a decrease in skin friction as the flow became more rarefied. This effect disappeared as the angle of the wedge increased. The relative decrease in skin friction became larger as the wedge angle increased.

Use of a modified temperature jump equation allowed the heat transfer to be calculated for the wedge. These results showed an increase in wall temperature, and a decrease in heat transfer, due to rarefaction effects. These effects were weakly dependent on the specific heat ratio of the gas, and strongly dependent on the Prandtl number and angle of the wedge.

References

[1]Hutchins, D. K., Harper, M. H., and Felder, R. L. "Slip correction measurements for solid spherical particles by modulated dynamic light scattering," *Aerosol Science and Technology*, Vol. 22, No. 2 , 1995, pp. 202-218.

[2]Braun, R. D., Wright, H. S., Croom, M. A., Levine, J. S., and Spencer, D. A. "Design of the ARES Mars Airplane and Mission Architecture", *Journal of Spacecraft and Rockets*, Vol. 43, No. 5, 2006, pp. 1026-1034.

[3]Sun, Q., Boyd, I. D., and Candler, G. V., "Numerical Simulation of gas flow over microscale airfoils," *AIAA Journal of Thermophysics and Heat Transfer*, Vol. 502 , No. 2, 2002, pp. 171-179.

[4]Mueller, T. J., and DeLaurier, J. D. "Aerodynamics of small vehicles," *Annual Review of Fluid Mechanics*, Vol. 35, 2003, pp. 89-111.

[5]Lin, T. C., and Schaaf, S. A. "Effect of Slip on Flow Near a Stagnation Point and in a Boundary Layer," NACA TN 2568, 1951.

[6]Maslen, S. H., "Second Approximation to laminar compressible boundary layer on flat plate in slip flow," NACA TN 2818, 1952.

[7]Kogan, M. N. *Rarefied Gas Dynamics*, Plenum Press, New York, 1969.

[8]Maslen, S. H. "Second-Order Effects in Laminar Boundary Layers," *AIAA Journal*, Vol. 1, No. 1, 1963, pp. 33-40.

[9]Van Dyke, M. "Higher Order Boundary Layer Theory," *Annual Review of Fluid Mechanics*, Vol. 1, 1969, pp. 265-292.

[10]Martin, M. J., and Boyd, I. D., "Momentum and Heat Transfer in a laminar boundary layer with slip flow," *AIAA Journal of Thermophysics and Heat Transfer*, Vol. 20, No. 4, 2006, pp. 710-719.

[11]Martin, M. J., and Boyd, I. D., "Stagnation point flow near the continuum limit," *AIAA Journal*, Vol. 47, No. 1, 2009, pp. 283-285.

[12]Arkilic, E B. Schmidt, M. A., and Breuer, K. S. "Gaseous slip flow in long microchannels," *Journal of MicroElectromechanical Systems*, Vol. 6, No. 2, 1997, pp. 167-178.

[13]Harley, J. C., Huang, Y. F., Bau, H. H., and Zemel, J. N. "Gas-Flow in Microchannels," *Journal of Fluid Mechanics*, Vol. 284, No. 1, 1995, pp. 257-274.

[14]Blasius, H. "Grezzschichten in Flüssigkeiten mit kleiner Reibung*", Zeitschrift für Mathematik und Physik,* Vol. 56, No. 1, 1908, pp. 1-37.

[15]Falkner, V. M., and Skan, S. W. "Solutions of the boundary-layer equations," *Philosophical Magazine*, Vol. 7, No. 12, 1931, pp. 865-896.

[16]Schlichting, H., and Gersten, K. *Boundary Layer Theory*, McGraw-Hill, New York, 2000.

[17]Maxwell, J. C. "On Stresses in Rarefied Gases Arising from Inequalities of Temperature," *Philosophical Transactions of the Royal Society of London*, Vol. 170, 1879, pp. 231-256.

[18]Incropera, F. P., and DeWitt, D. P. *Fundamentals of Heat and Mass Transfer*, Wiley, New York 2001.

[19]Smoluchowski von Smolan, M. "Über Wärmeleitung in verdünnten Gasen," *Annalen der Physik und Chemi*, Vol. 64 , No. 1, 1898, pp. 101-130

[20]White, F., *Viscous Fluid Flow*, 2nd ed., McGraw-Hill, New York, 1991, pp. 276-282.